J. Physiol. (1980), **308**, *pp.* 159–184
With 11 *text-figures*
Printed in Great Britain

CURRENT–VOLTAGE RELATIONS IN THE ROD PHOTORECEPTOR NETWORK OF THE TURTLE RETINA

BY D. R. COPENHAGEN* AND W. G. OWEN†

From the Departments of Physiology and Ophthalmology, University of California, San Francisco, California 94143, U.S.A.

(*Received 3 December 1979*)

SUMMARY

1. Electrical coupling between rod photoreceptors was studied in the eyecup preparation of the snapping turtle, *Chelydra serpentina*, using intracellular micro-electrodes.

2. The spatial profiles of rod responses to a long narrow slit of light were determined. The peak response amplitudes were found to decline exponentially as the slit was moved from the most sensitive position in the receptive field of each rod. The mean length constant was 55·7 μm.

3. Rods were simultaneously impaled in pairs and electrical coupling was demonstrated between the rods in seventeen of these pairs. No coupling was observed between rods separated by more than 110 μm. The transfer resistance, defined as the ratio of potential in the second rod (coupled potential) to the current injected into the first rod, varied from 0·2 to 13·2 MΩ.

4. The waveform of the coupled potential was time varying, exhibiting a peak and subsequent *relaxation phase*. The time course of the relaxation phase was voltage-dependent. At the cessation of current, the coupled potential rebounded beyond the resting potential and then decayed to the dark potential.

5. Plots of input current versus coupled potential showed strong outward-going rectification, chord transfer resistances being as much as 3·5 times lower for depolarizing currents.

6. Simultaneous impalements were made of pairs of neighbouring red-sensitive cones, of horizontal cells and rods, and of red-sensitive cones and rods. No evidence of coupling between cones and rods were found, nor could feed-back from horizontal cells onto rods be demonstrated; however, coupling between red-sensitive cones was found. This coupling exhibited neither the marked time-varying nor voltage-dependent properties that characterize the rod-rod coupling.

7. Individual rods were impaled with independent current passing and voltage sensing micro-electrodes. Pulses of current produced time-varying potentials having relaxation and rebound phases. Current–voltage measurements showed a strong outward-going rectification. Input resistances at the resting potential ranged up to 96 MΩ.

* Present address: Department of Ophthalmology, University of California, San Francisco, California 94143.

† Present address: Physiological Laboratory, Downing Street, Cambridge CB2 3EG, England.

0022-3751/80/2120-0646 $07.50

8. Square grid and hexagonal lattice models of ohmic electrical coupling were applied to the results. Using the measured values for the length constants and input resistances of single rods, we calculate that the plasma membrane resistance of each rod is approximately 1000 MΩ at the resting potential and that the coupling resistances are 272 and 444 MΩ for the square grid and hexagonal models, respectively.

9. The time-varying and voltage-dependent properties observed at the input and in the coupling between rods appear to reflect characteristics of the rod's plasma membrane and not of the coupling pathways between the rods. Both the outward-going rectification and relaxation phase of the response appear to involve voltage-dependent conductance increases in the rod's plasma membrane.

INTRODUCTION

Summative interactions between photoreceptors have been demonstrated in several vertebrate species. Individual photoreceptors respond not only to the light that strikes them directly, but also to the light that strikes neighbouring photoreceptors. The amplitude of the hyperpolarizing response in turtle cones is larger when light also strikes other cones within a radius of 60 μm (Baylor, Fuortes & O'Bryan, 1971). The response amplitude of the rods in the snapping turtle retina is similarly larger when photons are absorbed in other rods within a radius of 150 μm (Schwartz, 1973; Copenhagen & Owen, 1976*b*). Rods in the retina of the amphibian, *Bufo marinus* interact in a similar way (Fain, Gold & Dowling, 1976), and respond to light striking other rods up to 100 μm away (Leeper, Normann & Copenhagen, 1978; Gold, 1979).

Direct electrical coupling between photoreceptors appears to mediate the observed summative interactions. Baylor *et al.* (1971) showed that a turtle cone could be polarized by injecting current into another simultaneously impaled cone. Lasansky (1971) has shown direct anatomical contacts between cones in this same retina and has thus demonstrated a possible pathway for such coupling. In *Chelydra serpentina*, Copenhagen & Owen (1976*a*) demonstrated that current injected into a rod could polarize a second, simultaneously impaled rod. Although morphological contacts between rods in *Cheyldra* have yet to be demonstrated, the coupling is believed to be electrical on the basis of pharmacological experiments. Cobalt chloride, a potent blocker of chemical synaptic transmission, failed to disrupt the summative interactions between the rods when applied at concentrations that effectively blocked the chemically mediated, receptor-horizontal cell transmission (Schwartz, 1976; Owen & Copenhagen, 1977).

The functional characteristics of the individual rods are significantly affected by the electrical coupling. A step towards an understanding of these characteristics requires that the temporal and spatial properties of the interactions be determined. In this present paper we have studied the properties of the rod network by stimulating with light and by injecting intracellular currents. The first section of this paper describes the spatial profile of low-amplitude light-evoked responses in individually impaled rods. The subsequent section presents results from pairs of simultaneously impaled rods in which current was passed into one rod while the potential was

monitored in the other. Temporal, voltage-dependent and spatial properties of these coupled potentials are described. Finally, the input current–voltage properties of single rods are presented. Square grid and hexagonal lattice models of rod-rod coupling are used in analysing the results and the significance of the time-varying and voltage-dependent properties of the electrical coupling is discussed in terms of these models.

Our findings complement those recently reported by Detwiler, Hodgkin & McNaughton (1978), who demonstrated that the kinetics of rod responses to weak stimuli depend in an unexpected way upon the spatial distribution of the light, a result that also reflects time-varying, voltage-dependent properties of the rod's plasma membrane.

METHODS

Retinal preparation

Intracellular recordings were obtained from rod and cone photoreceptors, impaled with fine micro-electrodes (200–400 MΩ) advanced through the retina from the vitreal surface in an eyecup preparation of the snapping turtle, *Chelydra serpentina*. The eyecup was 'cemented' with Ringer-agar gel to the top surface of a Ag-AgCl indifferent electrode within a semi-enclosed chamber. Moistened O_2 or a mixture of O_2 and 5 % CO_2 was blown gently into the chamber to maintain the retinal tissue. All experiments were performed in a light-tight Faraday cage. Light stimulus patterns were provided by an optical system mounted on benching external to the cage. Further details of the dissection procedure, the electrodes, the optical system, and the recording apparatus are available in previous publications (Copenhagen & Owen, 1976*a*, *b*).

Receptive field profile measurements

In part of this study, a very narrow slit-shaped stimulating light was used to measure the receptive field profiles of individually impaled rods. This slit was constructed of razor blades glued to a glass microscope slide. The width of the reduced image of this slit, after being demagnified and projected onto the retina, was determined by moving it across the light-senstitive surface of a photomultiplier tube having a 5 μm diameter entrance pupil. Fig. 1 shows the photomultiplier output at different slit locations as the slit was moved across the entrance pupil in a direction perpendicular to its long axis. The distance between the points where the intensity was reduced to one half maximum was found to be 8 μm; this distance was taken as the nominal slit width.

Optics and micro-electrode positioning

Simultaneous penetrations of two rods were made with micro-electrodes whose tips were aligned prior to being advanced into the retina. A technique was devised in which an opaque dish, filled with saline, was placed over the chamber holding the eyecup. A 50 μm diameter stimulus spot was then focused on the top surface of the saline and the positions of the micro-electrode tips were adjusted so that they just penetrated the surface of the saline at the centre of the stimulus. In this way, the electrode tips were set within 50 μm of one another without the necessity of casting light onto the retina. The electrodes were then withdrawn several millimeters, the dish of saline removed and the retina raised to the level at which a briefly illuminated, annular stimulus was in sharp focus on the cone oil droplets. The micro-electrodes were then advanced through the vitreous into the retina.

Because of the low probability of simultaneously penetrating two rods, it became important to optimize the experimental protocol. For the results reported here we followed a standard sequence. Both micro-electrodes were advanced through the vitreous humour to a position about 50 microns proximal to the photoreceptors. One microelectrode was then advanced until a rod was impaled and identified. Rods were impaled about 180 μm distal to the inner limiting membrane, exhibited receptive field diameters of approximately 300 μm to flashed circular

stimuli, and produced a spectral sensitivity function that peaked at 520 nm; criteria which have been verified by intracellular injections of Procion yellow dye (Copenhagen & Owen, 1976*b*). The other micro-electrode was then advanced until a second rod was impaled. Following identification, a test for electrical coupling was made by passing pulses of current (1 to 6 $\times$ 10^{-9} A, 1 sec duration) into one of the rods while looking for voltage deflexions in the other rod. If the pulses of current produced a steady state voltage deflexion in the second rod, the cells were assumed to be coupled and the separation between the cells was immediately determined using the bar-shaped slit of light. Finally, the current–voltage characteristics of the couplings were measured in as much detail as time allowed. After this had been done, or if the micro-electrode slipped out of one of the rods into the extracellular space adjacent to it, a control experiment was performed by alternately passing pulses of current through each micro-electrode, while monitoring potential with the other micro-electrode.

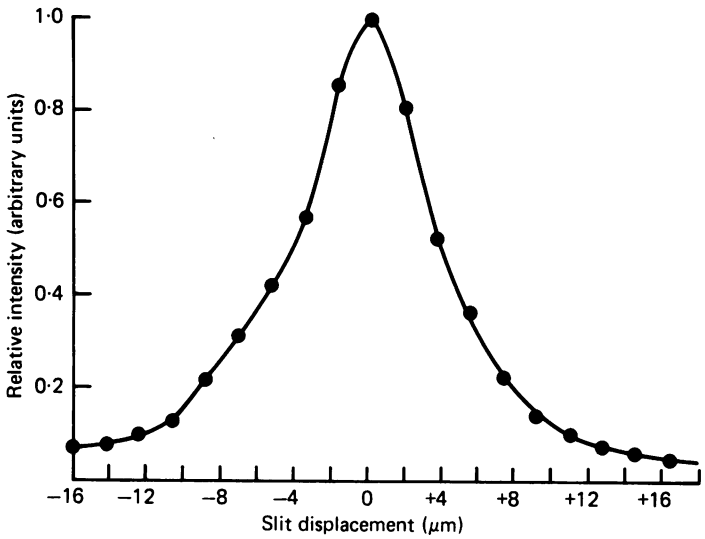

Fig. 1. Calibration of slit width. The long, narrow slit used to determine receptive field profiles was moved, in a direction perpendicular to its long axis, across the face of a 5 μm diameter circular aperture placed over the entrance pupil of a photomultiplier tube. The output of the photomultiplier tube is plotted as a function of slit displacement. The curve through the data points was drawn by hand. The nominal width of the slit is taken as 8 μm, which is well below ($< 1/5$) the minimum value for length constants measured in this study.

The distance between the two impaled rods was determined using a bar-shaped stimulus (27 μm $\times$ 800 μm) positioned and flashed at several points along a path perpendicular to its long axis.

Linear potentiometers were used to produce a voltage whose magnitude indicated the slit position. This voltage drove the x-axis of a storage oscilloscope while the rod's responses to each flash were displayed on the y-axis. The positions at which the maximum light responses were elicited in each rod were determined with the slit oriented first vertically and then horizontally. The distances between the maxima in the two directions were used to calculate the separation of the impaled rods. In several rod pairs, in which the separation was determined twice, the calculated values differed by less than 10 %.

Many times, cones and horizontal cells were impaled instead of rods. These cells were identified by their faster response waveform, peak spectral sensitivity and receptive field size; cone receptive fields never exceeded 150 μm in diameter while horizontal cell receptive fields ranged from a minimum of approximately 500 μm to greater than 1·5 mm in diameter. The cones and horizontal cells responded similarly to those in the retina of *Pseudemys scripta elegans* (Baylor *et al.* 1971; Fuortes & Simon, 1972; Lamb, 1976).

Electronic recording and data analysis

Potentials recorded by each micro-electrode were amplified by FET input preamplifiers (Winston Electronics, no. 1090) followed by DC amplifiers. These amplified signals were displayed on a storage oscilloscope and recorded on magnetic tape. The recording system time constant was approximately 10 msec with the input shunted to ground through 500 MΩ. Further details are described elsewhere (Copenhagen & Owen, 1976*b*).

The capacitative coupling between pairs of micro-electrodes varied with the distance of separation, and micro-electrode resistance. Although the magnitude of this capacitative coupling was never quantified, it was minimized by advancing the micro-electrodes from opposite sides of the eyecup and by prefiltering the current pulses through a single stage low pass filter having a time constant of approximately 40 msec (see controls, Fig. 3). Currents were passed into the rods by connecting a voltage source of variable magnitude to a 1000 MΩ resistance in series with the micro-electrode. Current was measured directly with a current-to-voltage converter ($\tau \simeq 10$ msec) placed between the indifferent electrode and ground. This direct method was chosen in order to eliminate uncertainties caused by possible changes in the micro-electrode resistance during current flow.

Input current–voltage measurement

Double-barrelled micro-electrodes were used in most of the current–voltage measurements in single rods. These electrodes were drawn on an air-blast micro-electrode puller from theta tubing having an outer diameter of 1·6 mm, a wall thickness of 0·3 mm and a septum width of 0·5 mm (Brown & Flaming, 1977). The single barrel resistances ranged between 150 and 300 MΩ in the optimized configuration used for penetration of receptors in the eyecup. Coupling resistances between barrels were typically 0·1–0·2 MΩ as measured in saline or in the vitreous. In some cases the coupling resistance was found to rise sharply and irreversibly (> 2 MΩ) as the electrode was advanced through the retina. Data taken with such electrodes were discarded.

RESULTS

Receptive field profile

The receptive field profiles of individually impaled rods were measured using a long narrow slit of light (8 μm × 800 μm) flashed at different positions across the retina. This type of stimulus pattern has two major advantages over earlier techniques which defined the receptive field properties in terms of light responses to concentric, circular spots centred upon the impaled rods (Fain *et al.* 1976; Schwartz, 1973, 1976; Copenhagen & Owen, 1976*b*). First, the need to centre the stimulus in two dimensions is obviated and secondly, the network analysis of responses to a one dimensional stimulus is simpler (Lamb, 1976; Nelson, 1977).

In Fig. 2 the peak response amplitude is plotted as a function of slit position for three different rods. On this log-linear plot it is clear that the data fall closely along the straight line and therefore are well approximated by the exponential relationship

$$E_p = k\, e^{-|x|/\lambda} \tag{1}$$

where E_p is the peak response amplitude, k is a constant, $|x|$ is the slit displacement and λ is the length constant. Table 1 lists the data from seven different rods. In this Table, V_{centre} is the peak response amplitude obtained when the slit was centred on the most sensitive region of the rod's receptive field. A simple exponential function was fitted to the data points in each direction away from slit position giving the maximum response. Using the method of least squares, $\lambda-$ and $\lambda+$ were derived for each rod. The correlation coefficients for $\lambda-$ and $\lambda+$ are given in Table 1. The mean length constant was 55·7 μm for the seven rods listed in Table 1. Both the

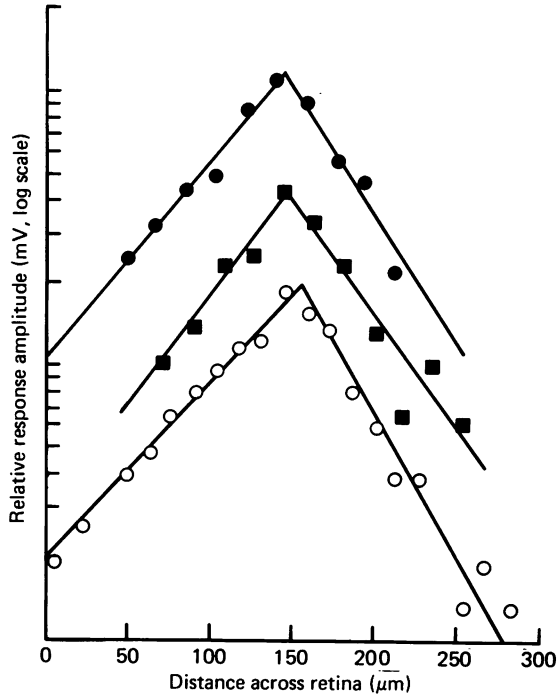

Fig. 2. Spatial profiles of three different rods. Three different impaled rods were stimulated by a long, narrow slit of light (8 μm × 100 μm) flashed at different positions across the receptive field of each cell. Each data point is based on the computer average of three to six individual responses. The straight lines were fitted by a least-squares regression method and represent simple exponential functions. The length constants were 60 and 48 μm for the top set of data, 52 and 65 for the middle set of data and 69 and 42 μm for the rod represented in the lowest set of data. All rods were stimulated with 40 msec flashes of 514 nm light.

TABLE 1. Length constants of rods measured with 8 μm × 800 μm slit of light. The responses on each side of the central point of the receptive field were fitted by the method of least squares to a simple exponential function. The length constants in each direction are given as $\lambda+$ and $\lambda-$. The correlation coefficients (r^2) in each direction are also listed. The peak response amplitude elicited when the slit was centered at the most sensitive part of the receptive field is given in the right-hand column

Rod	$\lambda+$ (μm)	r^2	$\lambda-$ (μm)	r^2	Vcentre (mV)
A	62·6	0·99	55·7	0·92	4·7
B	69·5	0·96	47·2	0·96	1·9
C	—	—	59·8**	0·65	0·9
D	52·0	*	67	0·96	1·2
E	60·4	0·98	46·9	0·94	1·8
F	51·3	0·94	58·6	0·91	1·3
G	52·8	0·97	54·5	0·84	2·1

* Only two data points. ** Only three data points.

mean constant and the individual length constants exceeded those reported for cones in *Pseudemys* (10–35 μm) (Lamb & Simon, 1976) and for rods of *Bufo marinus* (17–35 μm) (Leeper *et al.* 1978; Gold, 1979). In a previous study of snapping turtle rods, Schwartz (1975) estimated a length constant of 65 μm using a computed fit to responses elicited by concentric circular stimuli.

Two aspects concerning the shape of the spatial profile need mention. Lamb & Simon (1976) have reported that in *Pseudemys*, some rods exhibited a secondary peaking in amplitude as the slit was moved across the retina. We found no evidence for such a secondary peaking in this present study, an observation that might be explained by the higher density of rods in snapping turtle retina. Secondly, the two length constants, $\lambda-$ and $\lambda+$, were different for several of the rods. The greatest difference was in rod *B* for which $\lambda- = 69{\cdot}5$ *m* and $\lambda+ = 47{\cdot}2$ m. If the rods had been impaled near the edge of the retina in the inclined region of the eyecup, one might expect some differences attributable to defocusing of the slit pattern as it was moved across the retina. Every precaution was made to impale rods in the flatter, posterior regions of the eyecup, however (Copenhagen & Owen, 1976*b*). An alternative explanation is that the connexions between the rods might be anisotropic. Consistent with this physiological finding are anatomical observations of Golgi-stained rods which reveal that the teleodendria of peripheral rods are asymmetrical, tending to ramify towards the posterior pole of the retina (W. G. Owen, unpublished observations). Interestingly, however, the *average* length constant $((\lambda- + \lambda+)/2)$ remained fairly constant for all of the rods.

Coupled potentials: time varying properties

Thirty-seven pairs of rods were simultaneously impaled with microelectrodes during the course of this study: electrical coupling was demonstrated between the rods in seventeen of these pairs. This coupling was always of similar sign. Inward (hyperpolarizing) or outward (depolarizing) current always elicited a hyperpolarizing or depolarizing potential, respectively, in the coupled rod. Characteristically, the potential in the coupled rod (coupled potential) proved to be time-varying. Fig. 3 shows that in response to a current pulse, the coupled potential peaked and then relaxed to a steady-state level, closer to the resting potential. This exponential decline from the peak will be termed the *relaxation phase.*

The time constant of the decay of the potential during the relaxation phase varied with both the polarity and magnitude of the injected current. For small hyperpolarizing currents, this time constant was relatively large (> 500 msec) which produced a more rectangularly shaped coupled potential. As the magnitude of the hyperpolarizing currents increased, the relaxation time constants decreased to reach a minimum value of 200–300 msec. This is illustrated in Fig. 3 where the time constant decreased from 650 msec at 0·3 nA to 260 msec at $-1{\cdot}5$ nA. An interesting phenomenon, not illustrated in Fig. 3 but found in several other rod pairs, was that hyperpolarizing currents of even greater magnitude tended to produce relaxation phases with a lower time constant. Thus the coupled potentials sequentially exhibited a slower, then faster and finally a slower relaxation phase as the magnitude of the current was increased.

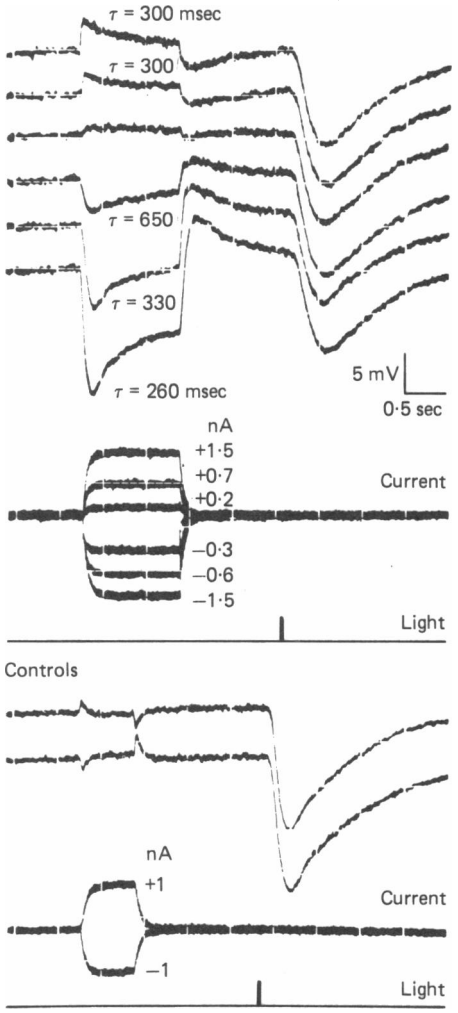

Fig. 3. Electrical coupling between two rods. Two rods were simultaneously impaled with micro-electrodes. With one micro-electrode serving as the current passing electrode, and another as the voltage sensing electrode, pulses of inward and outward current were passed into one of the rods. The wave forms of the current pulses, as measured in the ground return, are shown in the lower traces. The upper traces show first, the coupled potential induced by the current and secondly, the response to a large (> 750 μm diam.) flash of light. The time constants of the exponential decay of the coupled potential towards the steady-state level are shown adjacent to the appropriate records. The control records were obtained after the micro-electrode had been withdrawn from the first rod. Current pulses were passed through this micro-electrode into the extracellular space while recording the intracellular potential in the second rod.

The relaxation phase of depolarizing coupled potentials did not appear to vary as strongly with the magnitude of the current as did the hyperpolarizing potentials. The two higher-amplitude traces shown in Fig. 3 exhibited similar time constants of approximately 300 msec for input currents of +0·7 and +1·5 nA. The reduced magnitude of depolarizing coupled potentials made it difficult to measure accurately the time constants for all but the larger-magnitude currents in a few rod pairs. Generally the time constant ranged between 250 and 400 msec in these cells.

At the cessation of the current pulse, the coupled potential typically rebounded past the resting potential and then decayed to the resting potential. This *rebound phase* was evident for pulses of either polarity. After peaking, the potential decayed back to the resting potential with a time constant of about 500 msec.

It could be argued that the relaxation and rebound phases resulted either from capacitive coupling between the current and voltage micro-electrodes or from each of these micro-electrodes to ground. Indeed, in some of the early impalements of pairs of rods, a distinct capacitative artifact appeared in the coupled potentials. By maximizing the physical separation between the micro-electrodes, however, these capacitative artifacts were minimized, as is clearly shown in the control records of Fig. 3. Thus, the relaxation and rebound phases reflect the properties of the rod network.

The relation between coupled potential and input current

Extended measurements of the electrical coupling were performed on three rod-rod pairs. Results from one of these pairs are shown in Fig. 4, where the peak value of the coupled potential (filled circles) and steady state value (open circles), just prior to the termination of the current pulse, are plotted against injected current. The difference between the slopes of these two plots reflects the relaxation phase of the coupled potential. For hyperpolarizing currents of up to 2 nA, in all three pairs of rods, the relationship between the input current and coupled potential could be described satisfactorily by a linear function. However, for depolarizing potentials, this relationship proved to be markedly non-linear.

The current–voltage relationship showed strong rectification in all of the seventeen pairs of coupled rods: depolarizing currents produced smaller coupled potentials than hyperpolarizing currents of the same magnitude. Figs. 2 and 3 illustrate this rectification and show that it manifests itself both at the peak and throughout the relaxation phase. Although the degree of asymmetry in the current–voltage relationship varied among the rod-rod pairs, no correlation between the degree of rectification and the spatial separation of the rods was noted.

As a measure both of the degree of rectification and the strength of coupling between any two coupled rods we calculated the transfer resistance (R_T) (Jack, Noble & Tsien, 1975) which relates the input current to coupled potential. Specifically,

$$R_T = \frac{V_c}{I} \tag{2}$$

where V_c is the amplitude of the coupled potential with respect to the resting potential in the dark and I is the input current. Table 2 lists the transfer resistances

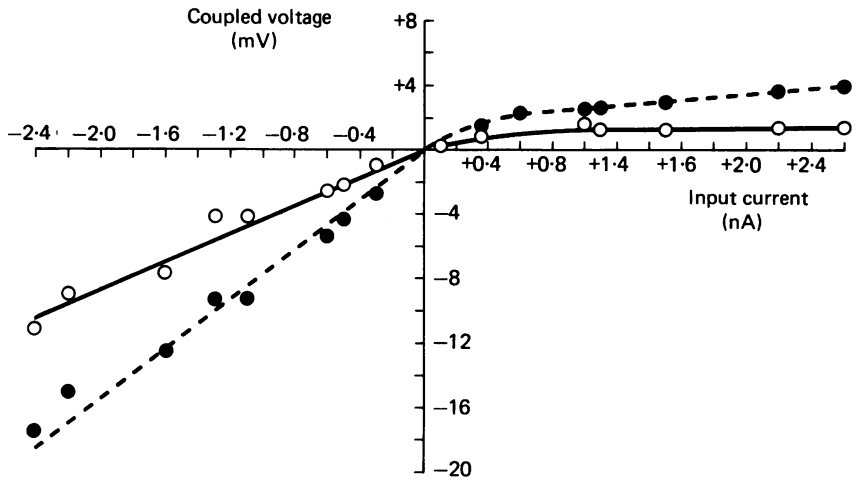

Fig. 4. Current–voltage characteristics of coupling between two rods. The abscissa plots the magnitude of hyperpolarizing (inward) and depolarizing (outward) pulses of current passed through one of the rods. The ordinate plots the resultant coupled voltage measured in the other simultaneously impaled rod. Filled circles show the magnitude of the peak voltage measured approximately 100 msec after the onset of the pulse while open circles plot the magnitude of the steady-state potential measured just prior to the termination of the current pulse. The curves for hyperpolarizing currents are straight lines having slopes of 7·6 mV/nA (7·6 MΩ) and 4·4 mV/nA (4·4 MΩ) respectively for the peak and steady state values of the coupled voltage. The curves for depolarizing currents were drawn by hand. Voltages are plotted with respect to the resting membrane potential in the dark. These rods were separated by a distance of less than 50 μm (R 16).

TABLE 2. Transfer resistances for three pairs of rods. These values are chord resistances determined by injecting strong pulses of outward (hyperpolarizing) and inward (depolarizing) current of approximately equal magnitude. The bracketed numbers give the value of the particular current used in each calculation. The *peak* values of the coupled potential have been used. The ratio (*H*/*D*) illustrates the magnitude by which the transfer resistances for hyperpolarizing currents exceeded those of the opposite polarity

Rod-rod Pair	Transfer resistances (MΩ) *Hyperpolarizing*	*Depolarizing*	Ratio (*H*/*D*)
14	8·70 (−0·85 nA)	2·5 (1·0 nA)	3·48
16	8·45 (−1·1 nA)	2·5 (+1·0 nA)	3·38
17	4·0 (−1·0 nA)	1·5 (+0·8 nA)	2·66

for hyperpolarizing and depolarizing currents in the three pairs of rods in which the more extensive current–voltage measurements were performed. The measure of the rectification is given by the ratio of the transfer resistances in the hyperpolarizing and depolarizing directions. This ratio ranged from 2·66 to 3·48 in these three rods.

Strength of coupling and rod-rod separation

An earlier study of the receptive field sizes of single rods showed that each rod is functionally connected to other rods separated by distances up to 150 μm (Copenhagen & Owen, 1976*b*). Since those previous results indicated that the responses of

a given rod were most strongly influenced by light absorption in its nearest neighbours, it was reasonable to suppose that the strength of coupling between rods, as measured by the simultaneous impalement of rod pairs, would similarly be greater between closer rods. Table 3 summarizes the coupling properties of the seventeen pairs of rods studied in this work. The separation distances were determined optically using the bar-shaped stimulus (see Methods) and ranged from 25 to 110 μm. Coupling was never observed between any two rods separated by more than 110 μm.

TABLE 3. Compilation of the separation distances, and transfer resistances, R_T, of the seventeen pairs of coupled rods. Separation was determined optically using two perpendicularly oriented bar-shaped stimuli moved across the retina (see Methods). R_T is the chord resistance calculated for input currents which hyperpolarized the rods from the resting membrane potential in the dark

Rod-rod pair	*Separation* (μm)	*Transfer resistance* (MΩ)	
		Peak	*Steady state*
1	—	0·2	—
2	50–100	1·8	0·6
3	50–100	1·4	0·6
4	—	1·4	0·3
5	<25	1·3	0·3
6	—	1·7	0·1
7	50	2·2	0·4
8	50	4·3	0·8
9	75–100	3·4	0·8
10	—	10	6·5
11	25	1·8	1·2
12	80	13·2	7·9
13	35	1·2	0·6
14	85	8·7	4·1
15	<50	0·6	0·3
16	<50	8·5	4·4
17	110	4·0	1·8

The transfer resistance, R_T, was used as a measure of the strength of coupling between any two rods; larger transfer resistances imply that the input current induced a larger potential in the coupled rod. The values of R_T, calculated for hyperpolarizing current pulses only, are listed in Table 3. Determinations of R_T were made at both the peak of the coupled potential and at the steady-state level. In the seventeen coupled pairs, the transfer resistances ranged from 0·2 to 13·2 MΩ at the peak and from 0·1 to 7·9 MΩ in the steady-state.

The separation distance correlated only moderately well with the transfer resistance between the coupled rods. In general, the closer rods exhibited higher transfer resistances and, hence, were more tightly coupled. However, a considerable variability was evident. In a similar study of coupling between horizontal cells in the dogfish, *Mustelus*, Kaneko (1971) reported variations in coupling ratios of more than 6:1 between cells believed to be directly adjacent to one another as determined by intracellular dye injections. Although some variability due to the effects of microelectrode impalement cannot be ruled out in the present study, our data are also consistent with the notion that the specific cell to cell connexions may be irregular. In the case of snapping turtle, the rods are distributed in irregular patterns across the retina (see Owen & Copenhagen, 1977). It is possible, therefore, that the actual

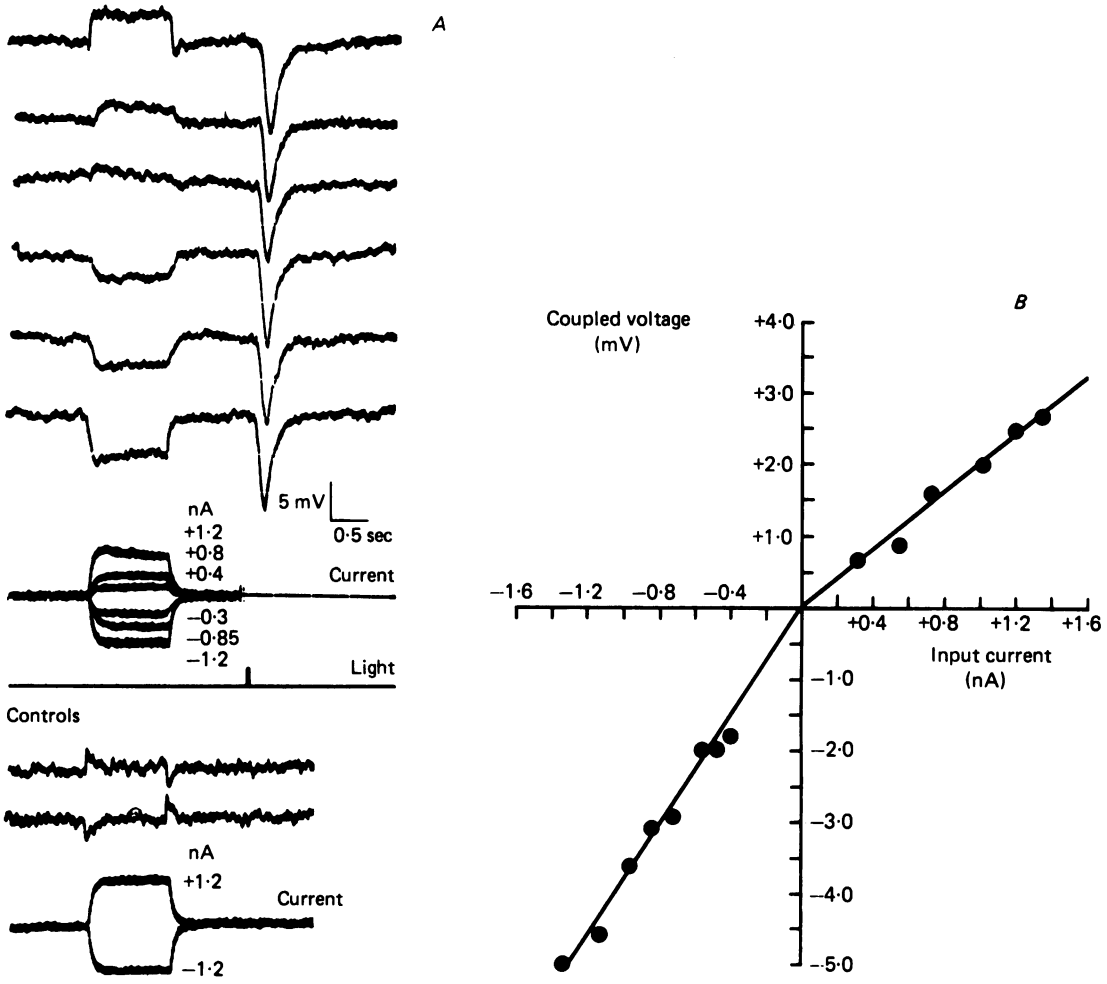

Fig. 5. Electrical couplings between red-sensitive cones. Two cones were simultaneously impaled with micro-electrodes and current pulses were passed into one of the cones in a manner similar to that described for rods. *A*. These tracings show the coupled potential induced by both inward and outward current pulses. The response to a flash of light (618 nm, 40 msec) follows the current pulse, *B*. The relation between current and coupled potential is plotted. Both depolarizing and hyperpolarizing potentials were well fitted by straight lines of different slopes. These cones were separated by approximately 40 μm.

magnitude of the coupling between any two cells may vary considerably, yet the total number of contacts, as judged by the constancy of the receptive field size, may vary much less. In this regard it is worth noting that we did impale two rods which, though only separated by 25 μm, were not electrically coupled to each other. Yet both of these cells had receptive field diameters in excess of 200 μm.

Simultaneous impalement of other retinal neurones

In the course of this study, simultaneous micro-electrode impalements were made in pairs of cones, pairs of horizontal cells and rods, and pairs of cones and rods.

Coupling between cells of each pair was studied in as much detail as possible. The cones of the snapping turtle were found to be electrically coupled in a manner similar to the cones of the related species, *Pseudemys scripta elegans* (Baylor *et al.* 1971). Simultaneous micro-electrode impalements were made in ten cone pairs; coupling was found between the cones in three of these pairs. The light responses in all coupled cones exhibited a maximum spectral sensitivity at wave-lengths greater than 600nm and were identified on this basis as red-sensitive cones. The coupled potential had the same sign as that induced in the cone into which the current was injected: there was no reversal of sign. Additionally, the coupling was reciprocal between the cones. Fig. 5*A* shows the coupled potential for depolarizing and hyperpolarizing current pulses of differing magnitudes. The coupled potential wave form was more rectangular than that in rods; the prominent relaxation and rebound phases were absent. Fig. 5*B* plots the current–voltage characteristics of coupling between two coupled cones. Linear functions of differing slopes satisfactorily fitted the data for the hyperpolarizing and depolarizing potentials. The reduced slope for outward currents is similar to the outward rectification observed between rods. The lesser degree of rectification in the cones is indicated by the lower ratio of transfer resistances: 1·95:1 in cones *vs.* a range of 2·6–3·5:1 in rods.

Simultaneous penetrations of rods and horizontal cells and of rods and cones revealed no evidence of coupling between neurones of these different classes. Seventeen rod-cone pairs were simultaneously impaled and, although the separations were not accurately determined in all these pairs, the rod and cone were separated by 25 μm or less in at least four pairs. Pulses of depolarizing and hyperpolarizing currents up to 4 nA were injected into both the rods and cones with no measurable deflection in the other photoreceptor. Nine rod-horizontal cell pairs were simultaneously penetrated and currents up to 6 nA passed into the horizontal cell evoked no detectable potential in the rods. This finding is consistent with our previous conclusion that there is no horizontal cell feed-back to rods in the snapping turtle retina (Owen & Copenhagen, 1977).

The input current–voltage relationship of the rod

The input current–voltage characteristics were studied in single rods impaled with separate current passing and voltage sensing micro-electrodes. In all experiments, save one double barrelled micro-electrodes (Brown & Flaming, 1978) were used. In one experiment, assessment of rod positions using vertical and horizontal slits of light revealed no spatial separation between the responses recorded from each micro-electrode. In addition, the transfer resistance between the 'two' rods exceeded any input impedance measured with double-barrelled electrodes. It was concluded that a single rod was impaled with two micro-electrodes. The results from this experiment, illustrated in Fig. 6, are particularly compelling since coupling between the barrels was minimized. Inward and outward current pulses of one second duration were passed into the rod impaled with the two independent micro-electrodes. The potential elicited in the rod showed many of the same characteristics observed in the coupled potentials. The relaxation and rebound phases can be discerned in these records although, partly because of the difference in scale, they appear less prominent here than in the coupled potentials of Fig. 3. The relaxation phase for inward currents

appeared most prominently in those records in which the rod was hyperpolarized by more than 5–10 mV, analagous to the behaviour of the coupled potentials. The time constant of the relaxation phase was approximately 250 msec for the −0·34 nA current. Other studies which examined the input current–voltage properties of rods have also revealed a relaxation phase in the voltage. Baylor & Fettiplace (1977) report a relaxation in the rods of *Pseudemys* and Bader, MacLeish & Schwartz (1978) and Werblin (1978) illustrate this phenomenon in the isolated rods of tiger salamander.

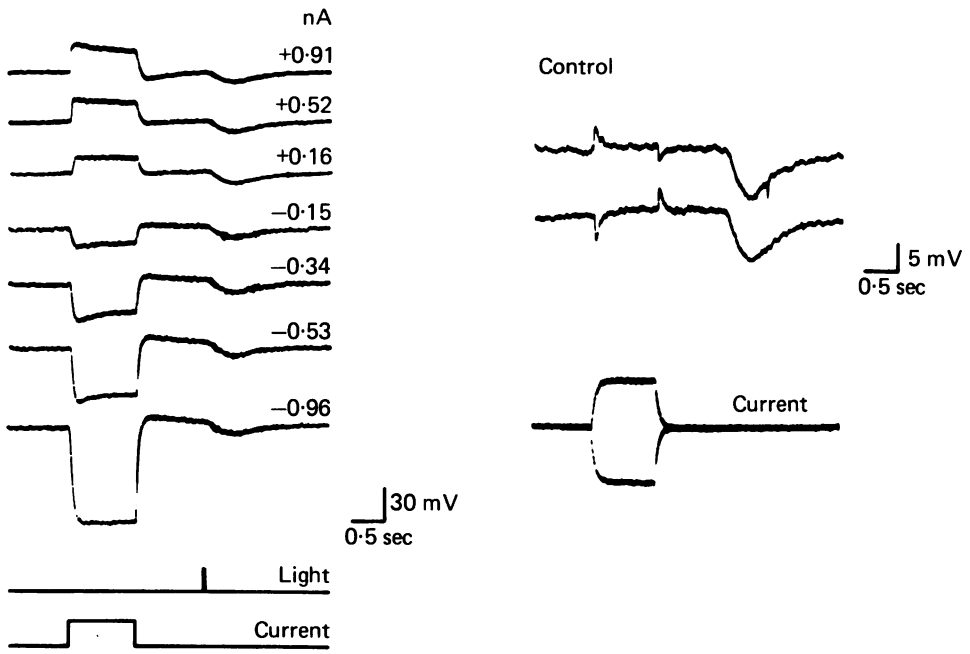

Fig. 6. Input current–voltage responses in a single rod. A rod was simultaneously impaled with two independently advanced micro-electrodes. Pulses of inward and outward current were passed through one micro-electrode and the resultant voltage deflexions were monitored with the second micro-electrode. The control records show the voltage deflexions after the current passing micro-electrode had been withdrawn to a position just adjacent to the rod. Light stimuli were delivered once every 5 sec (514 nm, 40 msec duration).

Fig. 7 plots the input current against voltage and shows that the outward rectification is very prominent in these rods. For the rod in Fig. 7, the chord resistance in the hyperpolarizing direction was 96 MΩ at the peak and 82 MΩ at the steady-state level (−0·51 nA) compared to 30·5 MΩ at the peak and 23·3 MΩ at the steady-state level (+0·91 nA) in the depolarizing direction. The ratio (H/D) at the peak in this rod was 3·18:1. Outward rectification of similar form was observed in all of the nine other rods studied with double barrelled micro-electrodes.

The effect of membrane polarization on the light response

Impaled rods were polarized by passing extrinsic current through the current passing micro-electrodes. The rods were stimulated with circular spots (750 μm diam.)

of light which covered the entire receptive field of these impaled cells. Hyperpolarizing the rod by as much as 50 mV below the resting potential produced a diminution of rather less than 15% in the amplitude of the light response. This is shown in Fig. 8*A* which illustrates the light response superimposed on current pulses of various magnitudes. Depolarizing the rod reduced the amplitude of the

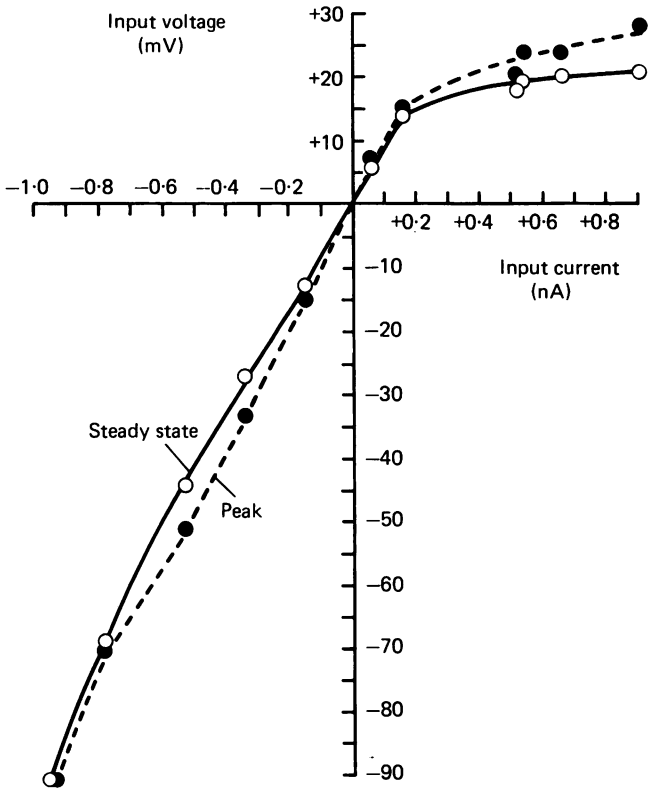

Fig. 7. Input current–voltage relationships of single rod. The magnitude of the voltage deflections in the rod shown in Fig. 7 are plotted against input current. Filled circles plot the value near the peak of the voltage wave form, (~ 100 msec) and open circles plot the value near the termination of the current pulse (~ 900 msec). The voltages induced by inward currents (of up to 0·5 nA) were fit by lines of slope 96 mV/nA (96 MΩ) at 100 msecs and 82 mV/nA (82 MΩ) at 900 msec. Potentials are plotted with respect to the resting membrane potential in the dark. The resting potential in this cell was −28 mV.

light responses to a much greater extent. For the rod in Fig. 8, a 25 mV depolarization (+0·97 nA) reduced the light response to less than 20% of the value at the resting potential. Previous studies have shown that depolarizing current, passed into photoreceptors of gecko (Toyoda, Nosaki & Tomita, 1969) or the rods of tiger salamander (Werblin, 1978; Bader *et al.* 1978) could reverse the direction of the light response. No reversal in the light response was observed in these present experiments for depolarizing currents up to +4 nA.

A surprising result is revealed when the data are plotted as in Fig. 8*B*. It will be noted that the two sets of data (see Figure legend) could be well fitted by a single

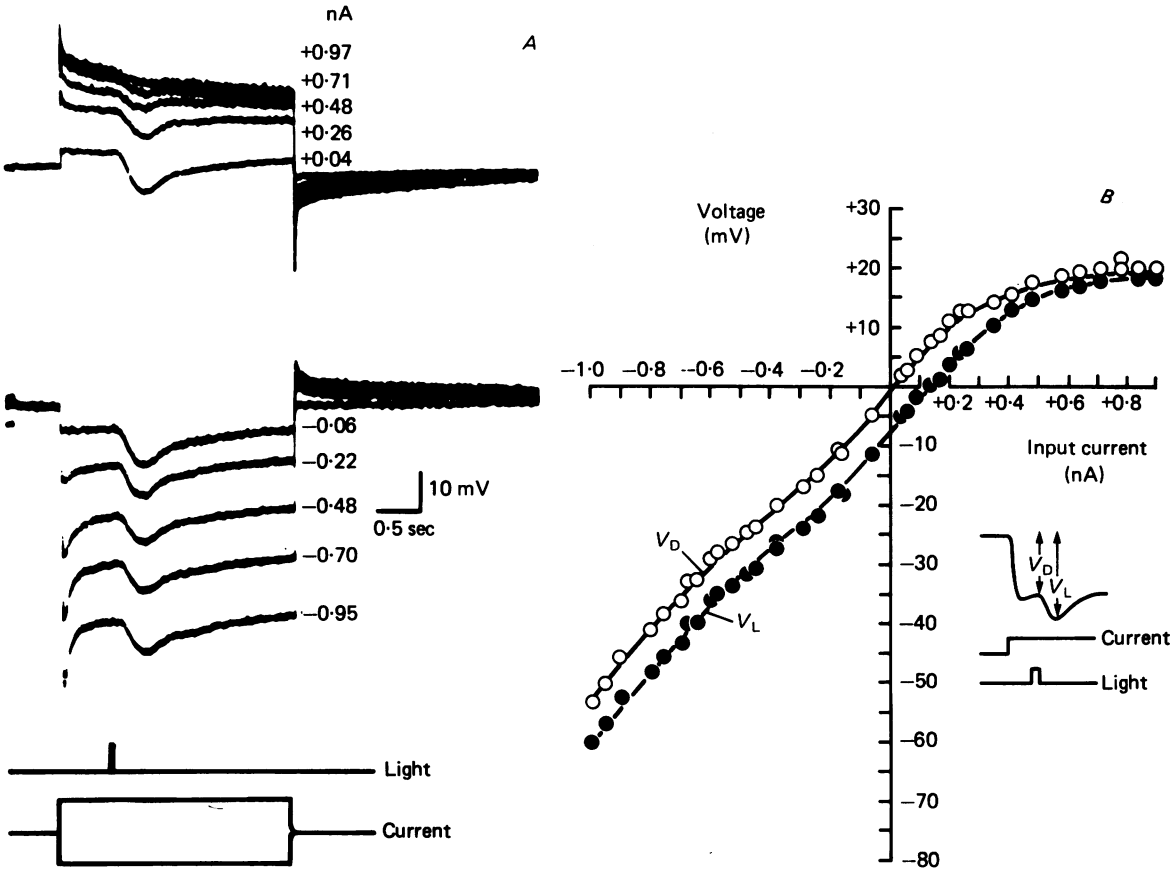

Fig. 8. Effects of membrane polarization on light responses. In a rod impaled with a double-barrel micro-electrode, extrinsic currents were used to polarize the rod in order to assess the effects upon the light response. *A*: these records show the voltages induced by inward and outward current pulses. A light, 750 μm in diameter, was flashed approximately 650 msec after the onset of the current pulse. *B*: plot of current–voltage relationship measured in the same rod. Open circles show the change in voltage, V_D, just before the light response. Filled circles show the total voltage change at the peak of the response to light V_C. A curve was drawn by eye through the open circles. The same curve, translated along the current axis, provides a good fit to the filled circles.

curve, translated laterally along the current axis. This was true for all the rods examined in this way. The significance of this result will be considered in the Discussion.

Light-induced reduction of input resistance and coupled potentials

In the rod that was impaled with two separate micro-electrodes, brief current pulses were passed during the light response in order to detect changes in the input resistance. Analysis of records such as that shown in Fig. 9 revealed that the magnitude of current-induced voltage, and hence resistance, was decreased by 29% immediately after the peak of the light response and recovered slowly as the cell

repolarized. In two pairs of simultaneously impaled rods, trains of current pulses were passed into one rod before and during the light response. The amplitude of the coupled potentials decreased approximately 15 % within 500 msec of the peak of the light response.

It should be mentioned that earlier attempts by us to measure resistance changes during the light response yielded mixed results. Using bridge techniques and single barrel micro-electrode impalement, we were unable to record consistently a significant resistance change during each response.

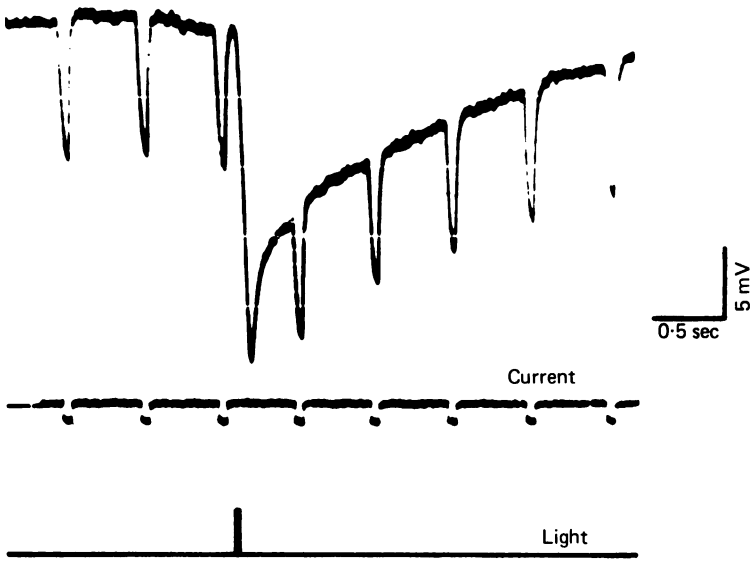

Fig. 9. Resistance change during light response. Brief, 80 msec, inward current pulses were passed into a rod at times before and during a light response. The amplitude of the voltage deflexion induced by these currents, measured with a second intracellular recording micro-electrode, declined immediately after the peak of the hyperpolarizing light response.

There are several published reports of light-induced changes in the input resistance of rods. Resistance decreases have been reported in tiger salamander (Lasansky & Marchiafava, 1974), mudpuppy (Werblin, 1975) and turtle (Schwartz, 1976). In the toad, *Bufo marinus*, Fain, Quandt, Bastian & Gerschenfeld (1978) showed that a light-induced resistance increase, while undetected in a normal Ringer could be unmasked by perfusing with one containing caesium. By contrast, Cervetto, Pasino & Torre (1977) report a resistance *increase* measured in the outer segments of rods in *Bufo bufo*. It seems likely, as Fain *et al.* have suggested, that the light-induced hyperpolarization of the rod triggers a voltage-dependent decrease in plasma membrane resistance associated with the relaxation phase of the response. If so, this voltage-dependent change may occur predominantly in the inner segment of the rod. The difficulty experienced in demonstrating a resistance change associated with the light response might be explained, in part, by the tendency of light-induced and voltage-dependent changes to cancel each other. The nature of the rod network

itself also makes detection of membrane resistance changes difficult. The voltage excursion produced by injection of a current pulse is proportional to the cell's input impedance. When cells are quite tightly coupled, a large change in the membrane impedance of all cells results in a relatively small change in input impedance and hence a relatively small change in voltage excursion. Such changes can easily be obscured by bridge or micro-electrode artifacts.

DISCUSSION

Resistive interconnexions between rods

The arguments supporting our conclusion that rods are interconnected by electrotonic junctions rather than chemical synapses have been presented in earlier publications (Copenhagen & Owen, 1976*b*; Owen & Copenhagen, 1977). Electrotonic junctions have been studied extensively in other systems. In some cases they have been shown to behave non-linearly, notably in crayfish giant axons (Furshpan & Potter, 1959) and between the embryonic cells of axolotl (Spray, Harris & Bennett, 1979). This is by no means the rule, however. The septal junctions in the giant axon of the earthworm were shown to behave as linear resistances with low associated capacitance (Brink & Barr, 1977). The junctions between supramedullary neurones of puffer fish were linear for voltage excursions of ± 50 mV (Bennett, Nakajima & Pappas, 1967).

What justification is there for assuming the junctions between rods to be linear rather than voltage-dependent? The observation that the coupled potential relaxes to a lower steady-state value during injection of a steady current pulse (Fig. 3), implies the existence of voltage dependent resistances in the plasma membrane of each rod, or in the coupling pathway itself. If such a resistance operated in the coupling pathway, a voltage-dependent resistance increase would be required to explain our observation. This would result in an increase in the input resistance of the rod into which current was injected and we would expect therefore to see an *increase* in polarization of that rod during the current pulse. This is not the case. A relaxation in potential is seen in the rod into which current is injected (see Fig. 6). This is the result we would expect if the voltage-dependent resistance were functionally located in the plasma membrane of each rod and the coupling pathway behaved in a linear (ohmic) manner.

Linear analysis of rod-rod coupling

In their analysis of the coupling between turtle cones, Lamb & Simon (1976) developed models of the cone network in which the cones were arranged in either square or hexagonal arrays, connected by linear resistors. By analysing these model networks they were able to relate the input resistance at a given node to the length constant and internodal distance. We have applied their solutions in our analysis of the rod network of the snapping turtle. Since these models are linear, they can only be applied to linear-range responses. Implications of membrane non-linearities will be discussed in a later section.

Fig. 10 illustrates a square lattice model of the rod network in which each rod is

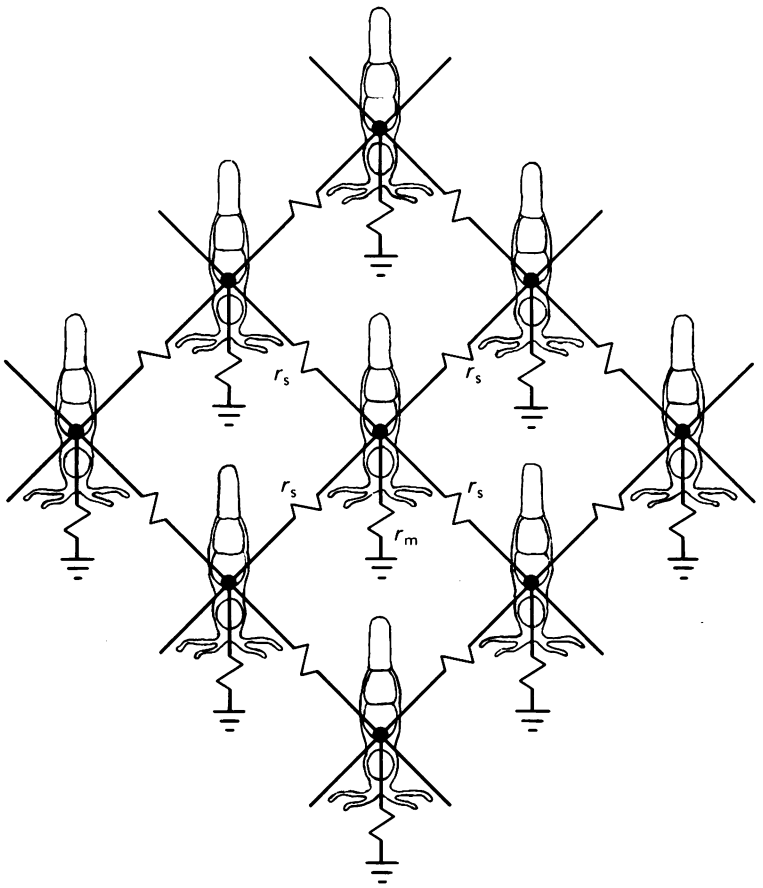

Fig. 10. Square lattice network of rod-rod coupling. The rods are assumed to be coupled to each of its four nearest neighbours by resistive pathways. The resistance of each connexion is given by r_s. The equivalent resistance across the plasma membrane of each rod is represented by r_m. The basal processes emanating from the synaptic pedicles of each rod are the presumed anatomical structures mediating electrical coupling between the rods as indicated schematically in the diagram.

connected to four neighbouring rods through a resistive pathway r_s. A membrane resistance, r_m, represents the lumped equivalent of the resistances across each rod's plasma membrane. In the present analysis, it is assumed that each rod is identical and that the resistances do not vary with voltage over the ranges tested. The specific solution for excitation of the network with a long, narrow slit follows the form

$$V_n = k e^{(-nD/\lambda)} \tag{3}$$

where

$$\gamma = \frac{r_s}{r_m} = 2\left(\cosh \frac{D}{\lambda} - 1\right) \text{ (Lamb \& Simon, eqn. (14}a\text{), 1976)} \tag{4}$$

with D being the mean rod to rod spacing, λ the length constant, V_n the peak voltage, and k a constant. The value of D was calculated from an examination of histological

material in which a large (90 μm × 210 μm) region of the retina was sectioned perpendicular to the long axis of the photoreceptors. This region contained thirty-two rods yielding a value of $D = 27{\cdot}9$ μm allowing for the 15% linear shrinkage of the preserved tissue. Using the measured mean value of $\lambda = 55{\cdot}7$ μm (Table 1), it is found that the ratio

$$\frac{r_s}{r_m} = 0{\cdot}255$$

Knowing the input resistance to any one rod it is possible to extend the calculations further to estimate the magnitudes of r_m and r_s. The input resistance to each rod in the square grid network is expressed by

$$r_{in} = V_{0,0} = r_m \frac{2}{\pi} \frac{\gamma}{\gamma+4} K\left(\left[\frac{4}{\gamma+4}\right]^2\right)$$

where $K(X)$ is the complete elliptical integral of the first kind (Lamb & Simon, 1976, eqn. (15); Abramowitz & Stegun, 1964). Thus

$$\frac{r_{in}}{r_m} = 0{\cdot}09$$

The input resistance of a single rod is taken as 96 MΩ, which is the chord resistance determined at the peak of the voltage response to current pulses (Fig. 7). Therefore,

$$r_m = 96/0{\cdot}09 = 1066 \text{ MΩ}$$

and hence

$$r_s = 272 \text{ MΩ}.$$

If a rod could be isolated from its neighbours, the instantaneous input resistance should be equal r_m and would thus be 1066 MΩ, an increase of approximately eleven-fold over the input resistance measured while the rod is in the network. In an earlier study, we estimated the ratio r_{in}/r_m from the ratio of the flash sensitivities measured with small (12 μm diam.) and large ($\geqslant$ 300 μm diam.) spots of light (Owen & Copenhagen, 1977). In that case a ratio of 13·5:1 was obtained, in good agreement with the ratio calculated using the square lattice model.

If it is assumed that rods are connected in a hexagonal arrangement, then, from Lamb & Simon (1977),

$$\frac{r_s}{r_m} = 0{\cdot}438$$

for $\lambda = 55{\cdot}7$ μm and $D = 27{\cdot}9$ μm. In order to estimate the ratio of r_{in}/r_m, we used computer calculations made by Dr Geoffrey Gold who has iteratively solved the equations for a hexagonal network. His analysis gives

$$\frac{r_{in}}{r_m} = 0{\cdot}095.$$

Thus

$$r_m = 96/0{\cdot}095 = 1015 \text{ MΩ}$$
$$r_s = 444 \text{ MΩ}.$$

In both cases the membrane resistance, r_m, of each rod is slightly greater than 1000 MΩ. The specific resistance can be calculated, knowing the total membrane

area of each rod. From histological sections we estimate that the surface area of snapping turtle rod outer segments is approximately 200 μm^2; the surface area of the remainder of the rod is approximately 1350 μm^2. Assuming a homogeneous plasma membrane, we calculate the specific resistance to be $\sim 1{\cdot}5 \times 10^4\ \Omega cm^2$. This value is considerably higher than that for squid axon ($1 \times 10^3\ \Omega cm^2$) but is consistent with the reported time constant of about 10 msec (Schwartz, 1976) assuming 1 $\mu F/cm^2$ as the membrane capacitance.

Applicability of the model

The parameters of the resistive network models used in this analysis were derived from measurements of small-amplitude responses. Although in three of the seven rods we noted a shortening in time-to-peak of responses as stimuli were laterally displaced, implying the existence of reactive elements in the network (Detwiler, Hodgkin & McNaughton, 1978), we found no systematic difference between the values of network parameters obtained from these rods and those obtained from the other four.

Anatomical evidence suggests that some rods may contact *more* than six other rods: up to ten teleodendria are seen to emanate from the rod pedicles. If each of these processes contacted another rod, the value of the coupling resistance calculated from the hexagonal model would represent a lower limit on the true value. The calculated value of the membrane resistance, on the other hand, would not be greatly in error.

The relaxation phase induced by inward currents and light

The results of this study are consistent with the idea that a voltage-dependent time-varying conductance increase underlies the relaxation phase observed during membrane hyperpolarization by light or current. The simplest explanation is that the hyperpolarization of the rod causes a conductance increase to one or more ions having an equilibrium potential more positive than the resting potential. By the arguments presented above, this conductance change must occur primarily in the plasma membrane of the rods rather than in the coupling pathway. The strongest evidence in support of the conductance increase is shown in Fig. 9 which illustrates a decrease in the input impedance of a rod following the peak hyperpolarization of the light response. Similar decreases have been reported by Schwartz (1976) in snapping turtle rods and by Lasansky & Marchiafava (1974) in tiger salamander rods. The action of caesium (Fain *et al.* 1978) mentioned earlier in the Results, also implies that response relaxation is associated with a conductance increase. Unfortunately it is not possible to make any useful estimate of the magnitude of this voltage dependent conductance change on the basis of instantaneous and steady-state current–voltage curves such as those of Fig. 7 since the relation between such curves is not straightforward (see Appendix).

With regard to the identity of the ionic species associated with the relaxation phase, however, it is worth noting that at the termination of inward current pulses strong enough to elicit a significant relaxation in voltage (Fig. 6), the rod membrane potential rebounds to a level several millivolts positive with respect to the resting potential. This strongly suggests that the ionic species involved has an equilibrium potential that is positive with respect to the resting potential. The rebound at termination of positive (outward) currents is consistent with this interpretation if we assume that the resting potential lies within the range of voltage-dependence of the conductance (i.e. some fraction of the channels are open at the resting potential).

The time constant of the relaxation phase, and presumably of the underlying conductance change was also found to be voltage-dependent, decreasing from ~ 500 to 200–300 msec as the rods were increasingly hyperpolarized from the resting potential.

Outward rectification

We believe the outward rectification observed in the coupled potentials and in the input current–voltage measurements to reflect a property of the plasma membrane of the rod. The arguments that support this belief depend on the linearity of the coupling resistances which was discussed earlier. Direct evidence favouring such a conclusion, however, is derived from recent results of recordings from isolated rods in which outward going rectification is a prominent feature of the input current–voltage characteristics (Bader *et al.* 1978; Werblin, 1978). It must be emphasized that such voltage-dependent behaviour as we observe in these experiments reflects only a fraction of that which exists in the plasma membrane, a consequence of the shunting effect of the network which tends to 'linearize' membrane non-linearities. We would expect, therefore, that the degree of outward rectification observed in an isolated, intact, rod would be many times greater than we report here. This outward rectification appears similar to the 'delayed rectification' found in squid axons (Hodgkin *et al.* 1952), in motoneurones (Ito & Oshima, 1965), and in other sensory receptor cells (Wiederhold, 1977). In the squid, delayed rectification results from a voltage-dependent increase in the membrane permeability to K ions (Hodgkin *et al.* 1952). Although Grundfest (1966) has observed that the delayed rectification in other systems can be caused also by an activation of the chloride conductance, strong support for the notion that the outward rectification in rods is at least partially due to changes in the potassium conductance is provided by Fain, Quandt & Gerschenfeld (1977). They reported that TEA, a blocker of voltage-dependent potassium channels, reduces the outward rectification in *Bufo* rods.

The effect of injected current on the light response

In Fig. 8*B*, it was noted that the current–voltage curve determined at the peak of the light response was well fitted by that measured in the steady-state just before illumination, when the latter was translated along the current axis by a fixed amount. This would suggest that the photocurrent measured in a rod is independent of the membrane potential over the range examined. Such would be the case if each rod behaved as a constant current generator. This would be consistent with the recent suggestion that the outer segments of isolated rods behave as light modulated constant current generators over a wide range of membrane potentials (Bader, MacLeish & Schwartz, 1979). If this were true it would contribute to the reasons for our failure to reverse the light response.

We are indebted to Professor Kenneth T. Brown for overall encouragement and support and to Drs J. Ashmore, G. Gold and H. Leeper for valuable discussions. We wish also to thank Drs P. McNaughton and G. Fain for helpful comments on the manuscript. This work was supported by U.S.P.H.S. grants EY-01801 to K. T. Brown, EY-001869 to D.R.C. and EY-001875 to W.G.O.

APPENDIX

The circuit shown in Fig. 11 is a highly simplified representation of the rod membrane. The light dependent conductance, g_2, we shall consider to be fixed during current injection in darkness. E_1 and E_2 have fixed values. The conductance, g_1, is a function of voltage and time and is assumed to obey first order kinetics. The extrinsic current flowing across the rod membrane is i, net flow being zero when the membrane is at the resting potential.

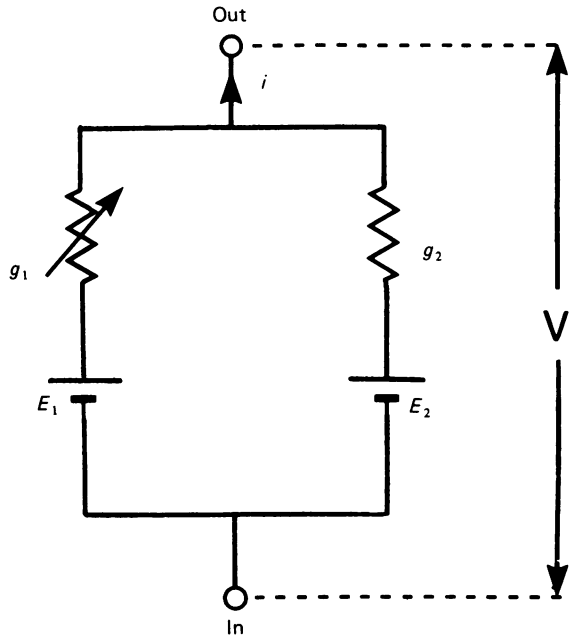

Fig. 11. Simplified model of a cell whose membrane contains a time-varying, voltage-dependent conductance g_1, a fixed conductance g_2 and associated equilibrium potentials E_1 and E_2. Extrinsic current i may be injected. The potential difference across the membrane is V. The capacitance of the cell membrane is neglected.

Current injection will displace the membrane potential by ΔV. We define the chord conductance, G_c, by

$$G_c = \frac{i}{\Delta V} \tag{1}$$

The slope conductance, G_s, is defined by

$$G_s = \left(\frac{\partial i}{\partial V}\right)_t \tag{2}$$

where t denotes time.
The circuit equation is

$$i = g_1 (V - E_1) + g_2 (V - E_2). \tag{3}$$

At the resting potential, $i = 0$ and

$$V_{rest} = \frac{\bar{g}_1 E_1 + g_2 E_2}{\bar{g}_1 + g_2} \tag{4}$$

where $\bar{g}_1$ is the initial, 'resting', value of g_1.
Differentiating eqn. (3) w.r.t. V gives the slope conductance

$$\left(\frac{\partial i}{\partial V}\right)_t = (V-E)\left(\frac{\partial g_1}{\partial V}\right)_t + (g_1)_t + g_2. \tag{5}$$

In the limit, as $t \to 0$

$$\left(\frac{\partial i}{\partial V}\right)_{t\to 0} = (\bar{g}_1 + g_2) \tag{6}$$

This is the *instantaneous slope conductance* of the membrane. Also, from eqn. (3), the *instantaneous chord* conductance is given by

$$\frac{i}{\Delta V} = (\bar{g}_1 + g_2). \tag{7}$$

Thus, we see that the instantaneous chord and slope conductances of the membrane should be equal. This is intuitively obvious when one remembers that g_1 is a function of time as well as of voltage and that following a voltage change a finite time must elapse before its value will be appreciably changed. If we allow such a change to occur the conductances will assume their new steady state values.

From eqn. (3) the *steady-state slope* conductance will be

$$\left(\frac{\partial i}{\partial V}\right)_{t\to\infty} = (g_1^\infty + g_2) + (V^\infty - E_1)\left(\frac{\partial g_1}{\partial V}\right)_{t\to\infty} \tag{8}$$

where g_1^∞ and V^∞ are steady-state values. Also from equation (3) the *steady-state chord* conductance can be obtained. Writing

$$i = (\bar{g}_1 + \Delta g_1)(V^\infty - E_1) + g_2(V^\infty - E_2)$$

we obtain

$$\frac{i}{\Delta V} = (\bar{g}_1 + g_2) + \frac{\Delta g_1 (V^\infty - E_1)}{\Delta V} \tag{9}$$

Comparing eqns. (7) and (9) we see that the steady-state chord conductance may be greater than the instantaneous chord conductance when either (i) E_1 is more negative than V^∞ and Δg_1 negative, or (ii) E_1 is more positive than V^∞ and Δg_1 is positive. Thus the relative magnitude of instantaneous and steady-state chord conductances cannot be used to estimate size or direction of the voltage-dependent, time-varying conductance change. One must know the value of E_1 before this can be determined.

Eqn. (7), on the other hand, indicates that determination of the *instantaneous* chord conductance by injection of brief current pulses should reveal changes in g_1. This technique was used in experiments of the kind illustrated in Fig. 9. As $\bar{g}_1$ changes during the light response so the magnitude of the voltage deflexions will change. In our case, the picture is complicated by the light induced decrease in g_2 and the coupling of the rods in an electrotonic network. These two factors combine to explain why the observed change in instantaneous input chord conductance is so small. The voltage-dependent increase in g_1 during the light response is likely to be considerably larger than such measurements indicate.

REFERENCES

ABRAMOWITZ, M. & STEGUN, I. A. (1964). *Handbook of Mathematical Functions*. New York: Dover.

BADER, C. R., MACLEISH, P. R. & SCHWARTZ, E. A. (1978). Responses to light of solitary rod photoreceptors isolated from tiger salamander retina. *Proc. natn. Acad. Sci. U.S.A.* **75**, 3507–3511.

BADER, C. R., MACLEISH, P. R. & SCHWARTZ, E. A. (1979). A voltage clamp study of the light response in solitary rods of the tiger salamander. *J. Physiol.* **296**, 1–26.

BAYLOR, D. A. & FETTIPLACE, R. (1977). Kinetics of synaptic transfer from photoreceptors to ganglion cells in turtle retina. *J. Physiol.* **271**, 425–448.

BAYLOR, D. A., FUORTES, M. G. F. & O'BRYAN, P. M. (1971). Receptive fields of cones in the retina of the turtle. *J. Physiol.* **214**, 265–294.

BENNETT, M. V. L., NAKAJIMA, Y. & PAPPAS, G. D. (1967). Physiology and ultrastructure of electronic junctions. I. Supramedullary neurons. *J. Neurophysiol.* **30**, 161–179.

BRINK, P. & BARR, L. (1977). The resistance of the septum of the median giant axon of the earthworm. *J. gen. Physiol.* **69**, 517–536.

BROWN, K. T. & FLAMING, D. G. (1977). New micro-electrode techniques for intracellular work in small cells. *Neuroscience* **2**, 813–827.

CERVETTO, L., PASINO, E. & TORRE, V. (1977). Electrical responses of rods in the retina of *Bufo marinus*. *J. Physiol.* **267**, 17–52.

COPENHAGEN, D. R. & OWEN, W. G. (1976*a*). Coupling between rod photoreceptors in a vertebrate retina. *Nature, Lond.* **260**, 57–59.

COPENHAGEN, D. R. & OWEN, W. G. (1976*b*). Functional characteristics of lateral interactions between rods in the retina of the snapping turtle. *J. Physiol.* **259**, 251–282.

DETWILER, P. B., HODGKIN, A. L. & MCNAUGHTON, P. A. (1978). A surprising property of electrical spread in the network of rods in the turtle's retina. *Nature, Lond.* **274**, 562–565.

FAIN, G. L., GOLD, G. H. & DOWLING, J. E. (1976). Receptor coupling in toad retina. In *Cold Spring Harb. Symp. quant. Biol.* **40**, 547–561.

FAIN, G. L., QUANDT, F. N. & GERSCHENFELD, H. M. (1977). Calcium-dependent regenerative responses in rods. *Nature, Lond.* **269**, 707–710.

FAIN, G. L., QUANDT, F. N., BASTIAN, B. L. & GERSCHENFELD, H. M. (1978). Contribution of a caesium sensitive conductance to the rod photoresponse. *Nature, Lond.* **272**, 467–469.

FUORTES, M. G. F. & SIMON, E. J. (1974). Interactions leading to horizontal cell responses in the turtle retina. *J. Physiol.* **240**, 177–198.

FURSHPAN, E. J. & POTTER, D. D. (1959). Transmission at the giant motor synapses of the crayfish. *J. Physiol.* **145**, 289–325.

GOLD, G. H. (1979). Photoreceptor coupling in the retina of toad, *Bufo marinus*. II. Physiology. *J. Neurophysiol.* **42**, 311–328.

GRUNDFEST, H. (1966). Heterogeneity of excitable membrane: Electrophysiological and pharmacological evidence and some consequences. *Ann. N. Y. Acad. Sci.* **137**, 901–949.

HODGKIN, A. L., HUXLEY, A. F. & KATZ, B. (1952). Measurement of the current–voltage relations in the membrane of the giant axon of *Loligo*. *J. Physiol.* **116**, 424–448.

ITO, M. & OSHIMA, T. (1965). Electrical behaviour of the motoneuronal membrane during intracellularly applied current steps. *J. Physiol.* **180**, 607–635.

JACK, J. J. B., NOBLE, D. & TSIEN, R. W. (1975). *Electric Current Flow in Excitable Cells*. Oxford: Clarendon.

KANEKO, A. (1971). Electrical connexions between horizontal cells in the dogfish retina. *J. Physiol.* **213**, 95–105.

LAMB, T. D. (1976). Spatial properties of horizontal cell responses in the turtle retina. *J. Physiol.* **263**, 239–255.

LAMB, T. D. & SIMON, E. J. (1976). The relation between intercellular coupling and electrical noise in turtle photoreceptors. *J. Physiol.* **263**, 257–286.

LAMB, T. D. & SIMON, E. J. (1977). Analysis of electrical noise in turtle cones. *J. Physiol.* **272**, 435–468.

LASANSKY, A. (1971). Synaptic organization of cone cells in the turtle retina. *Phil. Trans. R. Soc.* **262**, 365–381.

LASANSKY, A. & MARCHIAFAVA, P. L. (1974). Light-induced resistance changes in retinal rods and cones of the tiger salamander. *J. Physiol.* **236**, 171–191.

LEEPER, H. F., NORMANN, R. A. & COPENHAGEN, D. R. (1978). Evidence for passive electronic interactions in red rods of the toad retina. *Nature, Lond.* **275**, 234–236.

NELSON, R. (1977). Cat cones have rod input: A comparison of the response properties of cones and horizontal cell bodies in the retina of the cat. *J. comp. Neurol.* **172**, 109–136.

OWEN, W. G. & COPENHAGEN, D. R. (1977). Characteristics of the electrical coupling between rods in the turtle retina. In *Vertebrate Photoreception*, ed. BARLOW, H. B. & FATT, P. New York: Academic.

SCHWARTZ, E. A. (1973). Responses of single rods in the retina of the turtle. *J. Physiol.* **232**, 503–514.

SCHWARTZ, E. A. (1975). Rod-rod interaction in the retina of the turtle. *J. Physiol.* **246**, 617–638.

SCHWARTZ, E. A. (1976). Electrical properties of the rod syncytium in the retina of the turtle. *J. Physiol.* **257**, 379–406.

SPRAY, D. C., HARRIS, A. L. & BENNETT, M. V. L. (1979). Voltage dependence of junctional conductance in early amphibian embryos. *Science, N.Y.* **204**, 432–434.

TOYODA, J., NOSAKI, H. & TOMITA, T. (1969). Light-induced resistance changes in single photoreceptors of *Necturus* and *Gekko*. *Vision Res.* **9**, 453–463.

WERBLIN, F. S. (1975). Regenerative hyperpolarization in rods. *J. Physiol.* **244**, 53–81.

WERBLIN, F. S. (1978). Transmission along and between rods in the tiger salamander retina. *J. Physiol.* **280**, 449–470.

WIEDERHOLD, M. L. (1977). Rectification in Aplysia statocyst receptor cells. *J. Physiol.* **266**, 139–156.